Interfacial evolution and mechanical behavior of explosively welded titanium/steel joint under subsequent heat treatment process

Tong Wu
Chunli Yang (wut_hit@126.com)
Harbin Institute of Technology

Research Article

Keywords: Ti/steel clad plates, Titanium, Mild steel, Explosive welding, Heat treatment

Posted Date: February 11th, 2022

DOI: https://doi.org/10.21203/rs.3.rs-1343617/v1

Abstract

The TA2/15CrNi3MoV clad plates were fabricated by explosive welding and then were heat-treated in the temperature range of 700-1000 ℃ for 30 min. Its microstructure and tensile strength were investigated and the results elucidated that the heat treatment process accelerated the interdiffusion of constituent elements (e.g., Fe, Ti and C) at the TA2/15CrNi3MoV interface, thus resulting in the formation of FeTi, Fe_2Ti and TiC. For the samples heat-treated at 700 ℃, a continuous TiC layer was generated at the TA2/15CrNi3MoV interface, which hampered the formation of FeTi and Fe_2Ti. However, for the samples heat-treated at 800 ℃, the continuous TiC layer was broken up, resulting in a significant increase in the Fe-Ti layer to 1.21 μm. This resulted in a dramatic drop in tensile strength to 329.2 MPa. For samples heat-treated in the temperature range of 900-1000 ℃, the thickness of the brittle Fe-Ti layer was increased dramatically, leading to a rapid drop in tensile strength.

1 Introduction

Clad plates have been increasingly designed due to their potential ability to combine the advantages of base and clad materials [1, 2]. For example, Ti/steel clad plates are not only having a high strength/density ratio and superb corrosion resistance, but also have low fabrication costs, which is widely used in pipes, vessels and marine equipment [3, 4]. However, due to the metallurgical incompatibility of titanium and steel, brittle intermetallic compounds (IMCs) are easily generated at the titanium/steel bonding interface, making it difficult to manufacture titanium/steel clad plates by conventional fusion welding methods. [5, 6]. In addition, owing to the mismatches in their mechanical properties (e.g., heat transfer and thermal expansion), massive residual stresses are produced in the Ti/steel interface region and deteriorate the bonding interface [7]. To avoid the residual stresses and brittle IMCs at the Ti/steel interface, rolling bonding [8], diffusion bonding [9], and explosive welding [10, 11] were employed to address this problem. Among these solid-state metal joining processes, explosive welding is a reliable technology to join titanium and steel due to its simple process and high quality [11].

Explosive welding (EXW) offers an efficient alternative to joining metallurgical incompatible materials [12, 13]. It produces a weld joint by highspeed collision of the flyer plate and the base plate caused by the vast energy of detonation [14, 15], as shown in Fig. 1(a). The explosive welding interface plays a crucial role in the mechanical properties of the clad plates. Previous papers [16] revealed that the explosively welded interface undergoes fast heating (10^9 K/s) and cooling (10^7 K/s), resulting melted zone generated at the explosively welded interface and hence a metallic bond is formed. The high rate of heating and cooling rate during explosive welding reduces the interdiffusion of atoms and hence minimizes the formation of intermetallic compounds at the explosively welded interface [17]. However, the explosive welding method is not ideal for complex geometric shapes [13, 18, 19]. Consequently, explosive welding is often used in combination with other welding methods, such as tungsten inert gas (TIG), laser beam welding (LBW) and electron beam welding (EBW) [13, 18, 19]. Zhang et al. [18] achieved the dissimilar laser welding of Ti alloy to steel by using the TA2/Q235 explosively welded clad plates. However, Wang et al. [19] reported that brittle intermetallic components such as FeTi and Fe_2Ti were formed at the TA10/Q345 explosively welded

interface during the electron beam welding of Titanium alloy and mild steel using the explosively welded TA10/Q345 transition joint.

During these various subsequent manufacturing processes, Ti/steel explosively welded interface may be exposed under high temperatures. Therefore, it is essential to study the heat treatment processing on Ti/steel explosive-bonded joint to reveal the temperature effects on the bonding interface. It was reported in the previous literature that brittle intermetallic components such as Fe_2Ti and FeTi were generated in the bonding interface owing to the interdiffusion of constituent elements [13, 19, 20]. These intermetallic compounds deteriorate the Ti/steel interface strength [21, 22]. Meanwhile, residual stresses are produced at the interface due to the mismatch in their mechanical properties [17]. However, the effect of heat treatment temperature on the explosively welded TA2/15CrNi3MoV clad plates is still unknown.

In this work, the influences of heat treatment temperature on the tensile strength and microstructure of the explosively welded TA2/15CrNi3MoV interface were studied. The microstructure evolution of the explosively welded TA2/15CrNi3MoV interface during the subsequent heat treatment process was systematically investigated, and the influence of heat treatment temperature on the tensile strength of the explosively welded TA2/15CrNi3MoV interface was carefully discussed.

2 Materials And Methods

In this investigation, the Ti/steel explosively welded clad plates were fabricated by commercial purity titanium (TA2) plates and mild steel (15CrNi3MoV) using explosive welding method. The TA2 plate was chosen as the flyer plate and the 15CrNi3MoV plate was chosen as the base plate during the explosive welding process. The comical composition of TA2 plate and 15CrNi3MoV plate are presented in Table 1. The dimensions of TA2 plate and 15CrNi3MoV plate were 370 mm × 70 mm × 75 mm and 370 mm ×70 mm × 8 mm, respectively. To relieve the internal stress of the explosively welded TA2/15CrNi3MoV clad plates, annealing treatment was performed at 550 ℃ for 1.5 hours. After annealing treatment, the explosively welded TA2/15CrNi3MoV interfaces were heat-treated in the furnace under argon atmosphere in the temperature range between 700 ℃ and 1000 ℃ for 30 min. Then, the explosively welded Ti/steel clad plates were cooled in the air. Samples for microstructures analysis and mechanical properties were sectioned from the central part of the clad plates using electric discharge machining, as shown in Fig. 1(b).

Table 1
Chemical compositions of TA2 plate and 15CrNi3MoV plate (weight percent %).

Alloy	C	Ti	Fe	Si	Mn	S	P	Cr	Ni	Mo	V
TA2	<0.01	Bal	<0.01	-	-	-	-	-	-	-	-
15CrNi3MoV	0.15	0.002	Bal	0.26	0.43	0.002	0.005	1.02	2.9	0.21	0.095

Ti/steel explosive welding interfaces were ground using emery papers and then polished using 50nm SiO_2 solution to characterize the microstructure. Microstructures of the explosively welded TA2/15CrNi3MoV clad plates were examined by a ZEISS, SUPRA55 scanning electron microscope (SEM) operated at 30KV, equipped with electron backscattered diffraction (EBSD). A transmission electron microscope (TEM) was

used to reveal the microstructure, and the samples for TEM observation were fabricated by focused ion beam (FIB). The width of IMCs was measured at various locations of the wave peak interface by the SEM-BSE examination. The IMCs, formed at the explosively welded TA2/15CrNi3MoV interface, were analyzed by X-ray diffraction (XRD). A series of tensile tests were conducted on AGXplus at room temperature to evaluate the bond strength of the explosively welded Ti/steel clad plates. Three samples were prepared from each parameter, then tested at a speed of 1.5 mm/min. Tensile tests samples were machined by electric discharge machining (EDM) with dimension schematized in Fig. 1(d). SEM/EDS was conducted to analyze the fracture surfaces of the specimens after tensile tests.

3 Results And Discussion

3.1 Microstructure of as-annealed TA2/15CrNi3MoV explosive welding interface

Fig .2 shows the SEM-BSE images of the as-annealed TA2/15CrNi3MoV explosive welding interface. It can be clearly observed that there was a typical wave structure at the explosively welded TA2/15CrNi3MoV interface, as shown in Fig. 2(a). Microstructures investigation also has shown vortex generated in the TA2/15CrNi3MoV interface region. Fig. 2(b) shows a vortex structure at the interface, where brittle IMCs and micro-cracks exist. The generation of IMCs at the explosively welded Ti/steel interface can be related to the intense impact during the explosive welding process. The intense collision induced by explosive welding will have led to rapid and severe plastic deformation in the interface region, promoting the heat generated at the interface [23–25]. Previous study [16] reported that the explosively welded interface undergoes fast heating and cooling, leading to the formation of melted zone at the interface. Zhang et al. [23] revealed that the melted zone at explosively welded Ti/steel interface mainly consisted of FeTi. In addition, during the rapid cooling process, the mismatch in mechanical properties (e.g., heat transfer and thermal expansion) between the base plate and the flyer plate caused micro-cracks generated at the interface. Previous studies indicated that the micro-cracks were restricted within the IMCs and did not expand into the base materials [17]. The elemental distribution maps of the vortex region are indicated in Fig. 2(c-d). Fe-Ti intermetallic compounds were detected in the vortex. The generation of Fe-Ti IMCs can be related to the heating generation and accumulation caused by the severe plastic deformation during the explosive welding process.

To determine the phase composition at the wave peak region of the explosively welded TA2/15CrNi3MoV interface, the phase structure of the various region of the interface was confirmed by TEM. Fig. 3(a-b) shows the fabrication procedure of the TEM lamella. It can be clearly observed that the TEM lamella was prepared by FIB in the explosively welded TA2/15CrNi3MoV interface. Fig. 3(c) shows the HAADF images of the wave peak interface region. At the interface region, two reaction layers existed, namely 2 and 3. Fig. 3(d-e) shows high-resolution TEM (HRTEM) images of layer 2 and layer 3. Analysis of HRTEM images by fast Fourier transform (FFT) showed that layers 2 and 3 were TiC and FeTi, respectively. The thickness of the FeTi and TiC were about 0.095μm and 0.118μm, respectively. The formation of the FeTi and TiC was mainly induced by explosive welding and annealed process, respectively [23, 26]. This will be analyzed in detail later in this

paper. Thus, for the as-annealed sample, the phases from the 15CrNi3MoV side to the TA2 side were α-Fe, TiC, FeTi and α-Ti, respectively.

Figure 4 shows the EBSD results of the wave peak region of the explosively welded TA2/15CrNi3MoV interface. The image quality (IQ) maps and inverse pole figure (IPF) images demonstrated two distinct grains on the steel side: equiaxed grains and elongated grains. The elongated Fe grains were mainly distributed in the steel side away from the explosive welding interface. In contrast, the equiaxed Fe grains were distributed primarily in the steel side near the interface. The elongated Fe grains were mainly caused by the severe plastic deformation during the explosive welding [27]. At the same time, heat generated and accumulated at the Ti/steel interface due to the rapid and severe plastic deformation [16, 23]. This deformation heating resulted in the recovery and recrystallization occurring at the explosive welding interface, and then the equiaxed Fe grains were generated, as shown in Figure 4. In addition, the annealing treatment also facilitated the recovery and recrystallization. Figure 4(c,f) shows the kernel average misorientation (KAM) maps of the interface, which reflects the dislocation density/local strains [3]. It can be found that a substantial number of local strains were distributed at the elongated Fe grains, while few amounts of local strains were distributed at the equiaxed Fe grains. The elongated grains experienced intense plastic deformation and contained a great number of local strains. However, at the equiaxed Fe grains, the local strains were sharply decreased due to the recovery and recrystallization.

3.2 Microstructure evolution of explosively welded TA2/15CrNi3MoV interface after heat treatment

Figure 5 shows the Back-scattered SEM images of the explosively welded TA2/15CrNi3MoV interface after different heat treatment processes. The microstructure of the TA2/15CrNi3MoV interface changed significantly with the elevation of the heating temperature. For the samples heat-treated at 700 ℃, a grey layer was formed at the interface. This reaction layer, which can be determined by Akbari Mousavi's [20] research, was β-Ti. According to these previous researches [10, 20], β-Ti stabilizer elements (e.g., Fe, Cr and Ni) diffused from the steel side to the titanium side during the heat treatment, resulting in a decrease in the phase transformation temperature of α-Ti to β-Ti. Hence, the β-Ti layer was produced at the interface after heat treatment. When the temperature of the heat treatment was increased to 800 ℃, continuous β-Ti layer and Widmanstatten α-β structure were generated at the TA2 side, as shown in Figure 5(c). On the TA2 side away from the explosively welded interface, the amount of β-Ti stabilizer was not enough to retain the β-Ti to natural temperature and hence the Widmanstatten α-β structure were generated. Continuing to increase the heat treatment temperature, the β-Ti layer at the interface became thicker. When samples were heat-treated at 1000℃, the SEM-BSE images clearly indicated that the Ti/steel explosive welding interface region consisted of several layers, as shown in Figure 5(h). The generation of these layers will be analyzed in detail later in this paper.

Figure 6 shows SEM-BSE images of the explosively welded TA2/15CrNi3MoV interface at higher magnification. For the samples heat-treated at 700 ℃, a continuous black reaction layer was generated at the interface. According to the TEM (see Fig. 3) results and previous studies [26, 28], it can be determined that this black layer was TiC. TiC was a diffusion barrier, which hampered the diffusion of Fe atoms from the

steel side to the titanium side [28–30]. Hence, the Fe-Ti IMCs (i.e., Fe_2Ti and FeTi) and β-Ti layer increased slowly when the heat treatment temperature was lower than 700 ℃. When the heat treatment temperature was 800 ℃, the TiC layer was broken and existed in a semi-continuous state. This indicated that the Fe atoms diffusion barrier was disappeared, and then the Fe-Ti IMCs increased sharply to 1.2 μm, as shown in Figure 6(c). For the samples heat-treated at the temperature of 1000 ℃, Fe-Ti IMCs were generated at the interface, which contained fine blocky TiC inside (see Figure 6(f)). At this condition, the explosively welded Ti/steel interface region can be divided into several different layers. The chemical compositions of different layers are presented in Table 2. Layer □ was mainly contained Fe atoms (95.99 at%), which indicated that this layer was α-Fe. Layer □ in Figure 6 was composed of Fe (65.93 at%), Ti (30.87 at%) and C (3.20 at%) and layer □ was composed of Fe (43.44 at%), Ti (51.98 at%) and C (4.58 at%), both of which contains tremendous of Ti and Fe atoms, indicating that Fe-Ti was existing on these layers and was the primary phase. Layer □ and layer □ were mainly contained Ti atoms, while the Fe atoms in layer □ (10.21 at%) were more than layer □ (4.18 at%). Combined with the SEM-BSE images of the interface, it can be predicted that layer □ and layer □ was β-Ti and β-Ti + α-Ti, respectively. Hence, the explosively welded TA2/15CrNi3MoV interface from the 15CrNi3MoV side to the TA2 side can be divided into five layers, namely a-Fe, Fe_2Ti, FeTi, β-Ti and α-Ti + β-Ti, as shown in Table 2.

Table 2
chemical composition of various phases in the 1000 ℃ heat-treated specimens (at%)

position	□	□	□	□	□
Ti	0.36	30.87	51.98	87.45	93.56
Fe	95.99	65.93	43.44	10.21	4.18
C	3.65	3.20	4.58	2.34	2.26
Potential phase	α-Fe	Fe_2Ti	FeTi	β-Ti	β-Ti + α-Ti

To investigate the chemical distribution in the Ti/steel interface, the Fe, Ti and C element distribution graphs across the interface were illustrated in Fig. 7. The line profiles of the Fe, Ti and C element distribution graph presents several platforms at the interface, proving the formation of IMCs. For the as-annealed sample, the line profile of Fe and Ti elements possesses a significant gradient, indicating that the diffusion of Fe and Ti elements was limited. For samples heat-treated at the temperature of 700 ℃, C enrichment was observed at the interface. This approved that the TiC layer was generated at the TA2/15CrNi3MoV interface. In contrast, this phenomenon was not observed in the processing temperature range of 800-1000 ℃. This may be attributed to the dissolve and broken-up of the TiC layer. It can be clearly observed that after the TiC layer broken-up, the diffusion distance of Fe atoms in titanium increased significantly [28–30]. For samples heat-treated at 1000 ℃, the Fe and Ti element distribution presented two platforms, indicating that the Fe-Ti IMCs generated at the interface.

The XRD patterns of the explosively welded TA2/15CrNi3MoV interface at different temperatures are shown in Fig. 8. The change of diffraction peak intensity reflects the change of corresponding phase content [3]. The as-annealed specimens show the typical diffraction peaks of α-Fe and α-Ti. After heat treatment, new

IMCs (e.g., FeTi, Fe_2Ti and TiC) were detected. For the samples heat-treated at 700 ℃, the diffraction peak intensities of Fe-Ti IMCs were small. In contrast, it can be clearly observed that for samples heat-treated at 800 ℃ and 1000 ℃, the FeTi and Fe_2Ti were the main IMCs at the explosively welded TA2/15CrNi3MoV interface. In addition, it can be observed that the diffraction peak intensities of FeTi and Fe_2Ti increased with the temperature, indicating that the content of FeTi and Fe_2Ti increased with temperature.

To determine the microstructure evolution of the explosively welded TA2/15CrNi3MoV interface after the subsequent heat treatment process, standard free Gibbs energy (ΔG^{θ}) changes with the temperature of the IMCs (i.e., TiC, FeTi and Fe_2Ti) should be considered [28, 31], as shown in Fig. 9. It can be observed that the formation of TiC was the lowest value of ΔG^{θ} in the temperature range of 200 ℃-1400 ℃. This implied that TiC is preferentially formed at the interface compared to the FeTi and Fe_2Ti. After the continuous TiC layer was generated, the formation of Fe-Ti IMCs (i.e., FeTi and Fe_2Ti) was hindered due to the continuous TiC layer hampered the diffusion of Ti and Fe atoms across the TA2/15CrNi3MoV interface [29, 30]. Hence, the generation of IMCs (i.e., TiC, FeTi and Fe_2Ti) in the Ti/steel interface can be divided into two stages.

For the as-annealed sample, there were two reaction layers (i.e., FeTi and TiC) generated at the TA2/15CrNi3MoV interface (see Fig. 3(c)). During the explosive welding, the intense plastic deformation of the welded materials caused substantial amounts of heat at the TA2/15CrNi3MoV interface. This leads to the formation of local melting zones at the TA2/15CrNi3MoV interface region, where FeTi were observed [23]. During the annealing process, the C element diffused from the steel side toward the Ti side and finally caused the formation of TiC [26]. Hence, the formation of FeTi and TiC at the TA2/15CrNi3MoV interface was mainly induced by explosive welding and stress-relief annealing treatment process, respectively.

The continuous TiC layer hampered the diffusion of constituent elements (e.g., Ti and Fe) across the bonding interface, which hindered the formation of Fe-Ti IMCs at the TA2/15CrNi3MoV interface [29, 30]. For the TA2/15CrNi3MoV interface heat-treated at the temperature of 700 ℃, continuous TiC hampered the formation of FeTi and Fe_2Ti, as shown in Fig. 6(b). For the TA2/15CrNi3MoV interface heat-treated in the temperature range of 800 ℃-1000 ℃, continuous TiC layer broken up, leading to the barrier of the formation of FeTi and Fe_2Ti at the interface disappeared, as shown in Fig. 6(c-f). Due to this reason, the thickness of FeTi and Fe_2Ti layer increased significantly with the temperature in the temperature range of 800 ℃-1000 ℃. According to previous studies, Fe-Ti IMCs were very hard and brittle, which deteriorated the combination of the explosively welded TA2/15CrNi3MoV interface. Furthermore, the increase of the β-Ti layer also confirmed the accelerated diffusion of Fe atoms after the TiC layer broke up.

3.3 Mechanical properties and fracture analysis

The tensile strength of the explosively TA2/15CrNi3MoV interface at different conditions is presented in Fig. 10. It can be observed that the tensile strength decreased with the increase in temperature. The tensile strength of the as-annealed samples was 385.3 MPa, which was the maximum tensile strength of the explosively welded TA2/15CrNi3MoV interface. For the TA2/15CrNi3MoV interface heat-treated at 700 ℃, the tensile strength slowly decreased to 329.2MPa, which was 14.56% lower than that of the as-annealed samples. However, when the temperature of heat treatment was 800 ℃, the tensile strength sharply

decreased to 247.3MPa, which was 35.82% lower than that of the as-annealed samples. It can be attributed to the substantial number of IMCs (i.e., TiC, FeTi and Fe_2Ti) was existed at the interface, which deteriorates the combination of the TA2/15CrNi3MoV interface. During the tensile tests, the stress concentration generated at the TA2/15CrNi3MoV interface due to the deformation mismatch between IMCs and base materials, which eventually caused the explosively welded Ti/steel interface to fracture under a lower load [21]. For samples heat-treated at 850 ℃ and 900 ℃, the tensile strength of the explosively welded TA2/15CrNi3MoV interface sharply decreased to 232.6 MPa and 222.9MPa, respectively, due to the increase of IMCs. When the temperature of the heat treatment was 1000 ℃, the thickness of the Fe-Ti IMCs at the bonding interface increased to 4.23 μm, leading to the tensile strength of the explosively welded TA2/15CrNi3MoV interface sharply decreased to 163.6 MPa.

Figure 11 shows the fracture surface of the explosively welded TA2/15CrNi3MoV clad plates. It can be clearly observed that all the tensile test samples are fractured in the Ti/steel interface. For the as-annealed samples, some bulk fragments were existed on the fracture surface, as shown in Figure 11(a). For specimen heat-treated in the range of 700-1000 ℃, the failure mechanism of the explosively welded TA2/15CrNi3MoV interface was the brittle fracture. Chemical compositions measured by EDS reveal that the fracture surfaces were mainly contained FeTi and Fe_2Ti.

4 Conclusions

Heat treatment of TA2/15CrNi3MoV explosive welding clad plates was performed in the temperature range 700-1000 ℃, for 30min. The microstructure morphology of the interface and tensile strength were investigated, and some conclusions could be listed below:

(1) Heat treatment process accelerated the interdiffusion of constituent elements, which facilitated the formation of FeTi, Fe_2Ti and TiC. For the Ti/steel interface heat-treated at the temperature of 700 ℃, the continuous TiC layer hampered the formation of Fe-Ti IMCs. For the explosively welded TA2/15CrNi3MoV interface heat-treated in the temperature range of 800 ℃-1000 ℃, continuous TiC broken up and the thickness of Fe-Ti IMCs increased sharply to 4.2 μm.

(2) The tensile strength of the explosively welded TA2/15CrNi3MoV interface decreased with higher heat treatment temperatures. At the temperature of 700 ℃, the tensile strength slowly decreased to 329.2MPa. At the temperature of 800 ℃, the tensile strength dropped sharply to 247.3 MPa due to the increase in number of brittle Fe-Ti IMCs at the TA2/15CrNi3MoV interface.

Declarations

Author contributions

Tong Wu: experiment, methodology, investigation, writing — original draft preparation. Chunli Yang: supervision, resources, validation, writing — reviewing.

Funding

This research did not receive any specific grant from funding agencies in the public, commercial, or not-for-profit sectors.

Availability of data and material

Yes, the data and material are available.

Ethical approval

Not applicable.

Consent to participate

Not applicable.

Consent for publication

Not applicable.

Competing Interests

The authors have no relevant financial or non-financial interests to disclose.

References

1. Ha JS, Hong SI (2016) Deformation and fracture of Ti/439 stainless steel clad composite at intermediate temperatures. Mater Sci Eng A 651:805–809. https://doi.org/10.1016/j.msea.2015.11.041
2. Carvalho GHSFL, Galvão I, Mendes R et al (2018) Formation of intermetallic structures at the interface of steel-to-aluminium explosive welds. Mater Charact 142:432–442. https://doi.org/10.1016/j.matchar.2018.06.005
3. Zhao Z, Tariq N, ul H, Tang J et al (2020) Influence of annealing on the microstructure and mechanical properties of Ti/steel clad plates fabricated via cold spray additive manufacturing and hot-rolling. Mater Sci Eng A 775:138968. https://doi.org/10.1016/j.msea.2020.138968
4. Chai X, yang, Pan T, Chai F et al (2018) Interlayer engineering for titanium clad steel by hot roll bonding. J Iron Steel Res Int 25:739–745. https://doi.org/10.1007/s42243-018-0106-3
5. Zhao Z, Tariq N, Tang H et al (2020) Microstructural evolutions and mechanical characteristics of Ti/steel clad plates fabricated through cold spray additive manufacturing followed by hot-rolling and annealing. Mater Des 185:108249. https://doi.org/10.1016/j.matdes.2019.108249

6. Li B, He W, Chen Z et al (2019) Influence of annealing on the microstructure, interfacial compounds and mechanical properties of hot rolling bonded Ti/steel clad plate with bimetallic interlayered steel and vanadium. Mater Sci Eng A 764:138227. https://doi.org/10.1016/j.msea.2019.138227
7. Kundu S, Sam S, Chatterjee S (2011) Evaluation of interface microstructure and mechanical properties of the diffusion bonded joints of Ti-6Al-4V alloy to micro-duplex stainless steel. Mater Sci Eng A 528:4910–4916. https://doi.org/10.1016/j.msea.2011.02.050
8. Yang D, Luo Z, Xie G, Misra RDK (2018) Effect of interfacial compounds on mechanical properties of titanium–steel vacuum roll-cladding plates. Mater Sci Technol (United Kingdom) 34:1700–1709. https://doi.org/10.1080/02670836.2018.1472911
9. Orhan N, Khan TI, Eroğlu M (2001) Diffusion bonding of a microduplex stainless steel to Ti-6Al-4V. Scr Mater 45:441–446. https://doi.org/10.1016/S1359-6462(01)01041-7
10. Yang X, Shi C, gen, Ge Y, heng, Sabuj MNH (2018) Comparison of microstructure and mechanical properties of titanium/steel composite plates by two manufacturing processes. J Iron Steel Res Int 25:347–356. https://doi.org/10.1007/s42243-018-0038-y
11. Ye C, Zhai W, Lu G et al (2021) Effect of Secondary Explosive Welding on Microstructure and Mechanical Properties of 10CrNi3MoV Steel-Based Composite Plates. Metall Mater Trans A Phys Metall Mater Sci 52:1568–1573. https://doi.org/10.1007/s11661-021-06190-z
12. Prasanthi TN, Kirana R, Saroja S (2016) Explosive cladding and post-weld heat treatment of mild steel and titanium. Mater Des 93:180–193. https://doi.org/10.1016/j.matdes.2015.12.120
13. Wu T, Yang C (2022) Influence of pulse TIG welding thermal cycling on the microstructure and mechanical properties of explosively weld titanium / steel joint. Vacuum 197:110817. https://doi.org/10.1016/j.vacuum.2021.110817
14. Akbari Mousavi SAA, Farhadi Sartangi P (2009) Experimental investigation of explosive welding of cp-titanium/AISI 304 stainless steel. Mater Des 30:459–468. https://doi.org/10.1016/j.matdes.2008.06.016
15. Zhang H, Jiao KX, Zhang JL, Liu J (2018) Microstructure and mechanical properties investigations of copper-steel composite fabricated by explosive welding. Mater Sci Eng A 731:278–287. https://doi.org/10.1016/j.msea.2018.06.051
16. Bataev IA, Lazurenko DV, Tanaka S et al (2017) High cooling rates and metastable phases at the interfaces of explosively welded materials. Acta Mater 135:277–289. https://doi.org/10.1016/j.actamat.2017.06.038
17. Song J, Kostka A, Veehmayer M, Raabe D (2011) Hierarchical microstructure of explosive joints: Example of titanium to steel cladding. 528:2641–2647. https://doi.org/10.1016/j.msea.2010.11.092
18. Gao Y, Di, Zhou JP, Zhang Y et al (2019) Two pass laser welding of TC4 titanium alloy and 304 stainless steel using TA2/Q235 composite interlayer. Mater Lett 255:126521. https://doi.org/10.1016/j.matlet.2019.126521
19. Wang T, Zhang F, Li X et al (2018) Interfacial evolution of explosively welded titanium/steel joint under subsequent EBW process. J Mater Process Technol 261:24–30. https://doi.org/10.1016/j.jmatprotec.2018.05.031

20. Akbari Mousavi SAA, Sartangi PF (2008) Effect of post-weld heat treatment on the interface microstructure of explosively welded titanium-stainless steel composite. Mater Sci Eng A 494:329–336. https://doi.org/10.1016/j.msea.2008.04.032
21. Li BX, Chen ZJ, He WJ et al (2019) Effect of interlayer material and rolling temperature on microstructures and mechanical properties of titanium/steel clad plates. Mater Sci Eng A 749:241–248. https://doi.org/10.1016/j.msea.2019.02.018
22. Yadegari M, Ebrahimi AR, Karami A (2013) Effect of heat treatment on interface microstructure and bond strength in explosively welded Ti/304L stainless steel clad. Mater Sci Technol (United Kingdom) 29:69–75. https://doi.org/10.1179/1743284712Y.0000000099
23. Chu Q, Zhang M, Li J, Yan C (2017) Experimental and numerical investigation of microstructure and mechanical behavior of titanium/steel interfaces prepared by explosive welding. Mater Sci Eng A 689:323–331. https://doi.org/10.1016/j.msea.2017.02.075
24. Ning J, Zhang L, jie, Xie M, xia et al (2017) Microstructure and property inhomogeneity investigations of bonded Zr/Ti/steel trimetallic sheet fabricated by explosive welding. J Alloys Compd 698:835–851. https://doi.org/10.1016/j.jallcom.2016.12.213
25. Wang S, Han X (2019) Investigation on Microstructure and Mechanical Properties of TA10–Q245R Composite Plate Formed by Explosive Welding. J Mater Eng Perform 28:4241–4251. https://doi.org/10.1007/s11665-019-04193-x
26. Wachowski M, Gloc M, Ślęzak T et al (2017) The Effect of Heat Treatment on the Microstructure and Properties of Explosively Welded Titanium-Steel Plates. J Mater Eng Perform 26:945–954. https://doi.org/10.1007/s11665-017-2520-2
27. Jiang HT, Yan XQ, Liu JX, Duan XG (2014) Effect of heat treatment on microstructure and mechanical property of Ti-steel explosive-rolling clad plate. Trans Nonferrous Met Soc China (English Ed 24:697–704. https://doi.org/10.1016/S1003-6326(14)63113-7
28. Chai X, yang, Chen G, Chai F et al (2019) Hot roll bonding between commercially pure titanium and high-strength low-alloy steel using Fe interlayer. J Iron Steel Res Int 26:1126–1136. https://doi.org/10.1007/s42243-019-00322-x
29. Yu C, Xiao H, Yu H et al (2017) Mechanical properties and interfacial structure of hot-roll bonding TA2/Q235B plate using DT4 interlayer. Mater Sci Eng A 695:120–125. https://doi.org/10.1016/j.msea.2017.03.118
30. Yang X, Guo K, Gao Y et al (2021) Effect of carbon content on interfacial microstructure and mechanical properties of a vacuum hot-compressed bonding titanium-steel composite. Mater Sci Eng A 824:141802. https://doi.org/10.1016/j.msea.2021.141802
31. Tadashi M, Toshio En, Kenji I (1990) Effects of Carbon Content on the Diffusion Bonding of Iron and Steel to Titanium. Isij Int 30:978–984. https://doi.org/10.2355/isijinternational.30.978

Figures

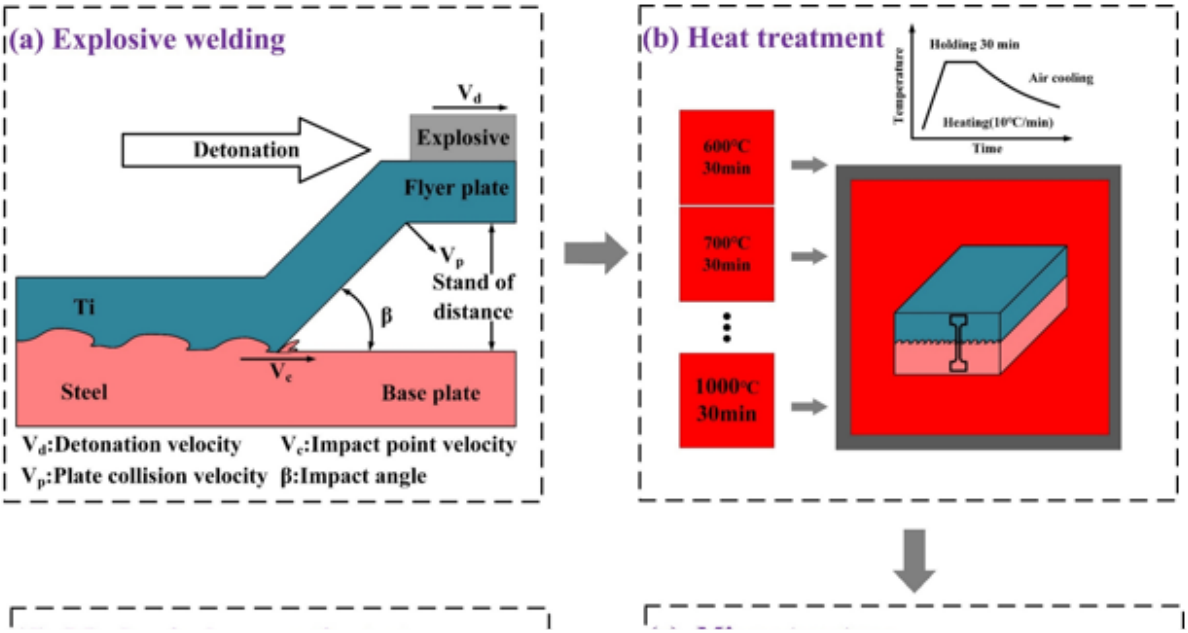

Figure 1

Process diagram of (a) explosive welding, (b) heat treatment processing, (c) microstructural characterization and (d) mechanical properties tests.

Figure 2

Back-scattered SEM images of the as-annealed TA2/15CrNi3MoV explosive welding interface: (a) wave morphology of the interface, (b) a vortex of the wave interface, (c) distribution of Ti and (d) distribution of Fe.

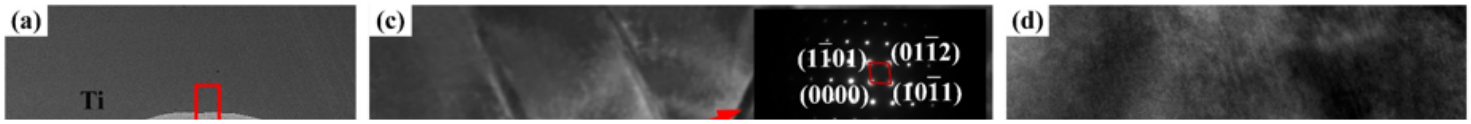

Figure 3

TEM results of as-annealed TA2/15CrNi3MoV explosive welding interface: (a) TEM sample cut from the TA2/15CrNi3MoV explosive welding interface and (b) prepared by FIB, (c) HAADF images, (d-e) HRTEM and FFT images at corresponding selected area.

Figure 4

EBSD analysis of the as-annealed Ti/steel interface: (a,d) IQ maps, (c,d) IPF maps, (e,f) KAM maps.

Figure 5

Back-scattered SEM images of the TA2/15CrNi3MoV interfaces heat treated at different temperature: (a) as-annealed, (b) 700 ℃, (c) 800 ℃, (d) 850 ℃, (e) 900 ℃, (f) 1000 ℃.

Figure 6

SEM-BSE images of the Ti/steel interface taken at higher magnification: (a) as-annealed, (b) 700 ℃, (c) 800 ℃, (d) 850 ℃, (e) 900 ℃, (f) 1000 ℃.

Figure 7

Element distributions across 15CrNi3MoV to TA2: (a) as-annealed, (b) 700 ℃, (c) 800 ℃, (d) 850 ℃, (e) 900 ℃, (f) 1000 ℃.

Figure 8

X-ray diffraction analyses of the explosive interface

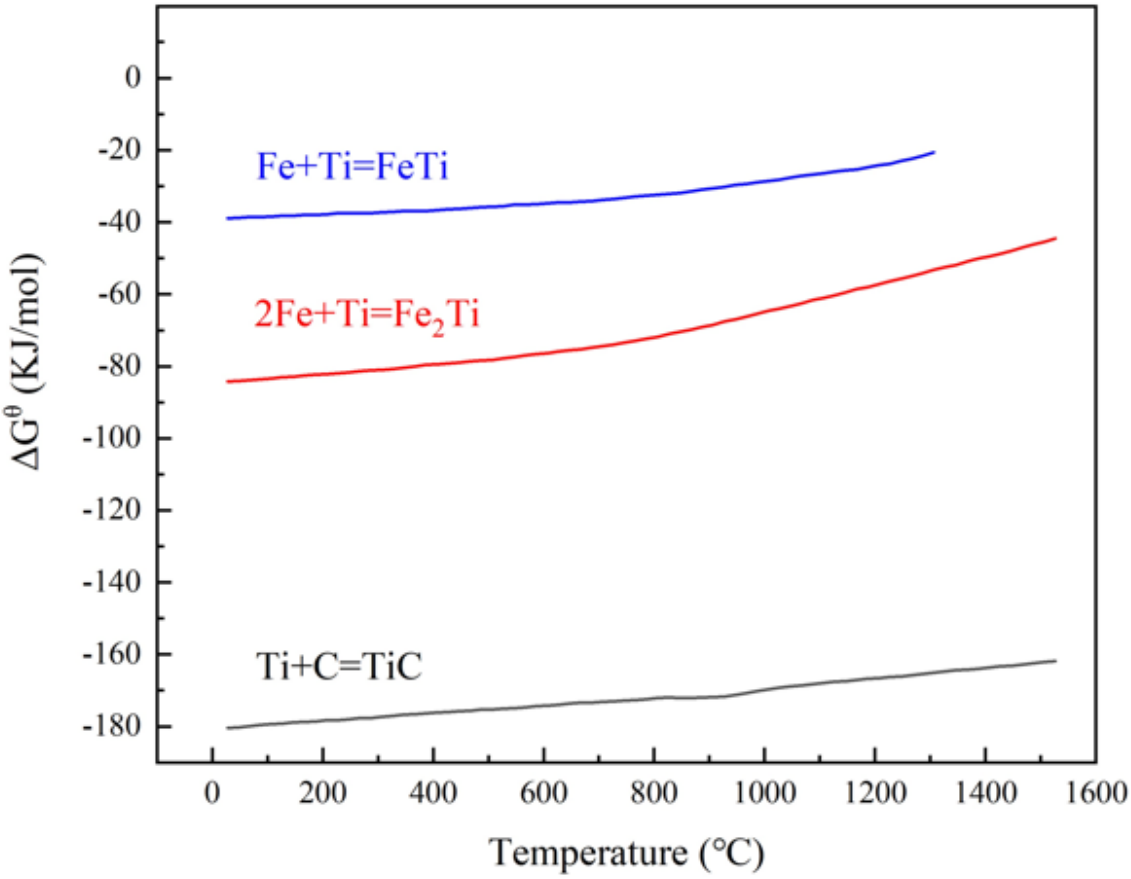

Figure 9

Standard free Gibbs energy change of TiC, FeTi and Fe_2Ti as a function of temperature [28,31].

Figure 10

Results of the tensile strength and thickness of IMCs at different conditions.

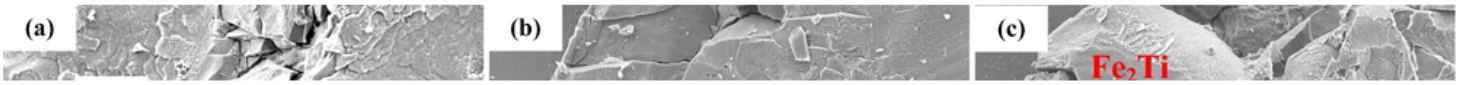

Figure 11

Fracture surface of TA2/15CrNi3MoV clad plates at different conditions: (a) as-annealed, (b) 700 ℃, (c) 800 ℃, (d) 850 ℃, (e) 900 ℃, (f) 1000 ℃.